

A Local-Adaptive Multiquadric Shape Parameter Applied with DRBEM to Convection-Diffusion Problem

Krittidej Chanthawara¹, Sayan Kaennakham^{2,3}

¹Department of Mathematics, Faculty of Science, UbonRatchathani Rajabhat University, UbonRatchathani, 34000, Thailand

²School of Mathematics, Institute of Science, Suranaree University of Technology, NakhonRatchasima 30000, Thailand

³Center of Excellence in Mathematics, Bangkok 10400, Thailand

sayan_kk@g.sut.ac.th

Abstract—While receiving more and more attention from scientists and engineers, the Dual Reciprocity Boundary Element Method (DRBEM) is known to face many factors and one of which is the choice of the Radial Basis Functions (RBFs) used. Amongst the popular choices of RBFs, the Multiquadric form is known to yield reliable solutions and yet, finding the optimal value of what is called ‘shape parameter’ noted, is known not to be straightforward. Nevertheless, it is well-known that the choice of the fixed value of is difficult to pinpoint and highly depends on the problem at hand. In this work, therefore, we propose a shape parameter that is a variable which can locally adapt itself correspondingly to the local change of the physics of the problem under investigation. For this reason, the convection-diffusion type of PDEs is focused on when the shape parameter is linked to the local Peclet number via the proposed formula. The results produced in this work show that the proposed shape variable is promising in producing satisfactory numerical solutions, particularly when compared with the fixed ones.

Index Terms—Boundary Element Method; Multiquadric; Variable Shape Parameter.

I. INTRODUCTION

Appearing as an alternative numerical method over the last two decades, the boundary element method (BEM) has become an important tool for solving a wide range of applied sciences and engineering that involve linear as well as specific types of nonlinear partial differential equations (PDEs). Amongst its appealing figures over the traditional methods of finite element, finite volume, and finite difference, BEM itself was facing the most challenging task when applied to nonlinear and/or time-dependence. An improved version of this scheme was proposed by Nardini and Brebbia [1] in 1982, and they named it as ‘Dual Reciprocity Boundary Element Method (DRBEM)’. In the process of DRBEM, the solution is divided into two parts: complementary solutions of its homogeneous form and the particular solutions of the inhomogeneous counterpart. Since the particular solutions are not always available especially in complex problems, the inhomogeneous term of the PDE is approximated by a series of simple functions and transformed to the boundary integrals employing particular solutions of the considered problem. The most widely used approximating functions in DRBEM are radial basis functions (RBFs) for which particular solutions can be easily determined [2].

The Radial Basis Functions (RBF), φ , are commonly

found as multivariate functions whose values are dependent only on the distance from the origin and commonly assumed to be strictly positive definite. This means that with $\mathbf{x} \in \Omega$ and $r \in \mathbb{R}^+$; or, in other words, on the distance from the point of a given set $\{\mathbf{x}_j\}$, and $\varphi(\mathbf{x} - \mathbf{x}_j) = \varphi(r_j) \in \mathbb{R}^+$ where can normally define as follows;

$$r = \|\mathbf{x} - \mathbf{x}^\ominus\|_2 = \sqrt{(x_1 - x_1^\ominus)^2 + (x_2 - x_2^\ominus)^2 + \dots + (x_n - x_n^\ominus)^2} \quad (1)$$

For some fixed points $\mathbf{x} \in \Omega$. Nevertheless, in this work, $r_j = \|\mathbf{x} - \mathbf{x}_j\|_2$ is the Euclidean distance and the radial basis function, φ , is chosen to be the Multiquadric type as firstly proposed by Hardy [3], defined as;

$$\varphi(r, \varepsilon) = \sqrt{\varepsilon^2 + r^2} \quad (2)$$

where ε is the so-called ‘shape parameter’ and is known to play a crucial role in determining the quality of the final results and has always been an open topic for decades. Hardy [3] suggests that by fixing the shape at $\varepsilon = 1/(0.815d)$,

where $d = \left(\frac{1}{N}\right) \sum_{i=1}^N d_i$, and d_i is the distance from the node to its nearest neighbour, good results should be anticipated. Also, in the work of Franke [4] where the choice of a fixed shape of the form $\varepsilon = \frac{0.8\sqrt{N}}{D}$ where D is the diameter of the smallest circle containing all data nodes, can also be a good alternative.

Some recent attempts to pinpoint the optimal value of ε involve the work of Zhang et al. [5] where they demonstrated and concluded that the optimal shape parameter is problem dependent. In 2002, Wang and Lui [6] pointed out that by analysing the condition number of the collocation matrix, a suitable range of derivable values of ε can be found. Later in 2003, Lee et al. [7] suggested that the final numerical solutions obtained are found to be less affected by the method when the approximation is applied locally rather than globally.

While the study of providing crucial and useful information of this shape parameter based on numerical aspect alone and/or fixed values is growing, it then appears that it may be

more useful to take into consideration also the physical aspect of the problem at hand. This idea is the initiative of this work and led to two primary objectives. Firstly, we implemented and applied the methodology of DRBEM to a problem containing a sudden change in local physical property and, for this, the convection-diffusion type is focused on. Secondly, we have proposed a new form of Multiquadric RBF shape parameter which behaves local-adaptively based on local changes in the Peclet number; the ratio of the contributions to mass transport by convection to those by diffusion. The results obtained from this investigation were validated against other alternative numerical works in literature when available.

II. THE DUAL RECIPROCITY BEM FOR CONVECTION-DIFFUSION PROBLEMS

The work aims to investigate two-dimensional convection-diffusion problems governed by the following equation numerically;

$$\frac{\partial u}{\partial t} + V_x \frac{\partial u}{\partial x} + V_y \frac{\partial u}{\partial y} = \omega_x \frac{\partial^2 u}{\partial x^2} + \omega_y \frac{\partial^2 u}{\partial y^2} - \beta u + g(x, y, t) \quad (3)$$

where V_x, V_y are convection coefficients, and ω_x, ω_y are diffusion coefficients. The last two terms; βu and the source term $g(x, y, t)$, are additional and needed only in specific cases.

By setting $\omega_x = \omega_y = \omega$, we obtain;

$$\frac{\partial u}{\partial t} + V_x \frac{\partial u}{\partial x} + V_y \frac{\partial u}{\partial y} + \beta u - g(x) = \omega \left(\frac{\partial^2 u}{\partial x^2} + \frac{\partial^2 u}{\partial y^2} \right) \quad (4)$$

Leading to;

$$\frac{1}{\omega} \left(\frac{\partial u}{\partial t} + \left(V_x \frac{\partial u}{\partial x} + V_y \frac{\partial u}{\partial y} \right) + \beta u - g(x) \right) = \frac{\partial^2 u}{\partial x^2} + \frac{\partial^2 u}{\partial y^2} \quad (5)$$

subject to the initial condition $u(x, y, 0) = \beta(x, y)$, with $(x, y) \in \Omega$ and the boundary condition $u(x, y, t) = \gamma(x, y, t)$. Where $x, y \in \partial\Omega$, $t > 0$ and Ω is a domain of the problem, $\partial\Omega$ is its boundary, β and γ are known functions.

The mathematical construction of the dual reciprocity boundary element method (DRBEM) can start with the Poisson equation as follows;

$$\nabla^2 u = b(x, y) \quad (6)$$

which its equivalent integral form, given by Nardini and Brebbia [1], is as follows;

$$c_i u_i + \int_{\Gamma} q^* u d\Gamma - \int_{\Gamma} u^* q d\Gamma = \sum_{j=1}^{N+L} \alpha_j \left(c_i \hat{u}_{ij} + \int_{\Gamma} q^* \hat{u}_j d\Gamma - \int_{\Gamma} u^* \hat{q}_j d\Gamma \right) \quad (7)$$

where u^* is the fundamental solution and the term \hat{q}_j is defined as $\hat{q}_j = \frac{\partial \hat{u}_j}{\partial \mathbf{n}}$, where \mathbf{n} is the unit outward normal to its boundary Γ , and can be written as follows;

$$\hat{q}_j = \frac{\partial \hat{u}_j}{\partial x} \frac{\partial x}{\partial n} + \frac{\partial \hat{u}_j}{\partial y} \frac{\partial y}{\partial n} \quad (8)$$

Next, we apply the boundary element method as explained in Chanthawara et al. [8], and with N and L is the number of boundary and internal nodes respectively, b can be now approximated by;

$$b_i(x, y) \approx \sum_{j=1}^{N+L} \alpha_j f_{ij}(x, y) \quad (9)$$

Here, the function f is the radial basis function which is, in this work, the multiquadric type and is to be detailed in the next section. With this radial basis function, we then have;

$$\nabla^2 \hat{u}_j = f_j \quad (10)$$

For some particular solution, \hat{u}_j .

Applying Green's theorem, the boundary element approximation to Equation (7), then it becomes, at node i^{th} ;

$$c_i u_i + \sum_{k=1}^N \int_{\Gamma_k} q^* u d\Gamma - \sum_{k=1}^N \int_{\Gamma_k} u^* q d\Gamma = \sum_{j=1}^{N+L} \alpha_j \left(c_i \hat{u}_{ij} + \sum_{k=1}^N \int_{\Gamma_k} q^* \hat{u}_j d\Gamma - \sum_{k=1}^N \int_{\Gamma_k} u^* \hat{q}_j d\Gamma \right) \quad (11)$$

For $i = 1, \dots, N$.

After introducing the interpolation function and integrating over each boundary elements, the above Equation (11) can be re-written regarding nodal values as;

$$c_i u_i + \sum_{k=1}^N H_{ik} u_k - \sum_{k=1}^N G_{ik} q_k = \sum_{j=1}^{N+L} \alpha_j \left(c_i \hat{u}_{ij} + \sum_{k=1}^N H_{ik} \hat{u}_{kj} - \sum_{k=1}^N G_{ik} \hat{q}_{kj} \right) \quad (12)$$

where the definition of the terms H_{ik} and G_{ik} can be found in Toutip [9]. The index k is used for the boundary nodes which are the field points. After application to all boundary nodes, using a collocation technique, Equation (12) can be compactly expressed in matrix form as follows;

$$\mathbf{Hu} - \mathbf{Gq} = (\mathbf{H}\hat{\mathbf{U}} - \mathbf{G}\hat{\mathbf{Q}})\alpha \quad (13)$$

By substituting $\alpha = \mathbf{F}^{-1}\mathbf{b}$ from Equation (9), into Equation (13) making the right-hand side of Equation (13) a known vector. Therefore, it can be rewritten as;

$$\mathbf{Hu} - \mathbf{Gq} = \mathbf{d} \quad (14)$$

where $\mathbf{d} = (\mathbf{H}\hat{\mathbf{U}} - \mathbf{G}\hat{\mathbf{Q}})\mathbf{F}^{-1}\mathbf{b}$. Applying boundary condition(s) to Equation (14), then it can be seen as the simple form as follow;

$$\mathbf{Ax} = \mathbf{y} \quad (15)$$

where \mathbf{x} contains N unknown boundary values of u 's and q 's .

After Equation (15) is solved using standard techniques such as Gaussian elimination, the values at any internal node can be calculated from Equation (15), i.e. $c_i = 1$ as expressed in Equation (12) where each one involves a separate multiplication of known vectors and matrices.

$$\begin{aligned} u_i &= -\sum_{k=1}^N H_{ik} u_k + \sum_{k=1}^N G_{ik} q_k \\ &= \sum_{j=1}^{N+L} \alpha_j \left(c_i \hat{u}_{ij} + \sum_{k=1}^N H_{ik} \hat{u}_{kj} - \sum_{k=1}^N G_{ik} \hat{q}_{kj} \right) \end{aligned} \quad (16)$$

We first substitute Equation (18) into Equation (17) to get the equation system matrix which is expressed as;

$$\mathbf{Hu} - \mathbf{Gq} = (\mathbf{H}\hat{\mathbf{U}} - \mathbf{G}\hat{\mathbf{Q}})\mathbf{F}^{-1}\mathbf{b} \quad (17)$$

Setting;

$$\mathbf{S} = (\mathbf{H}\hat{\mathbf{U}} - \mathbf{G}\hat{\mathbf{Q}})\mathbf{F}^{-1} \quad (18)$$

Then Equation (17) becomes;

$$\mathbf{Hu} - \mathbf{Gq} = \mathbf{Sb} \quad (19)$$

Now, getting back to the convection-diffusion governing equation, Equation (3), as described in Nee and Duan [10],

$V_x \frac{\partial u}{\partial x}, V_y \frac{\partial u}{\partial y}$ are approximated similarly, that is;

$$\left. \begin{aligned} V_x \frac{\partial u}{\partial x} &= \mathbf{V}_x \frac{\partial \mathbf{F}}{\partial x} \mathbf{F}^{-1} \mathbf{u} \\ V_y \frac{\partial u}{\partial y} &= \mathbf{V}_y \frac{\partial \mathbf{F}}{\partial y} \mathbf{F}^{-1} \mathbf{u} \end{aligned} \right\} \quad (20)$$

From Equation (20) and

$$b = \frac{1}{\omega} \left(\frac{\partial u}{\partial t} + \left(V_x \frac{\partial u}{\partial x} + V_y \frac{\partial u}{\partial y} \right) + \beta u - g(x) \right) \quad (21)$$

For the time derivative, the forward difference method is expressed as $\dot{u} = \frac{\partial u}{\partial t} = \frac{u^{t+1} - u^t}{\Delta t}$. Substituting Equation (20) and Equation (21) to Equation (19) and then;

$$\begin{aligned} \mathbf{Hu} - \mathbf{Gq} &= \mathbf{S} \left(\frac{1}{\omega} \left(\dot{u} + \left(\mathbf{V}_x \frac{\partial \mathbf{F}}{\partial x} \mathbf{F}^{-1} \mathbf{u} + \mathbf{V}_y \frac{\partial \mathbf{F}}{\partial y} \mathbf{F}^{-1} \mathbf{u} \right) + \beta \mathbf{u} - \mathbf{g}(\mathbf{x}) \right) \right) \end{aligned} \quad (22)$$

and then;

$$\begin{aligned} \mathbf{Hu} - \mathbf{Gq} &= \frac{1}{\omega} \mathbf{S} \left(\dot{u} + \left(\mathbf{V}_x \frac{\partial \mathbf{F}}{\partial x} \mathbf{F}^{-1} + \mathbf{V}_y \frac{\partial \mathbf{F}}{\partial y} \mathbf{F}^{-1} + \beta \mathbf{I} \right) \mathbf{u} - \mathbf{g}(\mathbf{x}) \right) \end{aligned} \quad (23)$$

with setting;

$$\mathbf{C} = \mathbf{V}_x \frac{\partial \mathbf{F}}{\partial x} \mathbf{F}^{-1} + \mathbf{V}_y \frac{\partial \mathbf{F}}{\partial y} \mathbf{F}^{-1} + \beta \mathbf{I} \quad (24)$$

Substituting Equation (24) in Equation (23). The following expressions are obtained.

$$\mathbf{Hu} - \mathbf{Gq} = \frac{1}{\omega} \mathbf{S} (\dot{u} + \mathbf{C}\mathbf{u} - \mathbf{g}(\mathbf{x})) \quad (25)$$

Let $\mathbf{R} = \frac{1}{\omega} \mathbf{S}$,

$$\mathbf{Hu} - \mathbf{Gq} = \mathbf{R} (\dot{u} + \mathbf{C}\mathbf{u} - \mathbf{g}(\mathbf{x})) \quad (26)$$

and then;

$$\left(\frac{\mathbf{R}}{\Delta t} + \mathbf{RC} - \mathbf{H} \right) \mathbf{u}^{t+1} + \mathbf{Gq}^{t+1} = \frac{\mathbf{R}}{\Delta t} \mathbf{u}^t + \mathbf{Rg}(\mathbf{x}) \quad (27)$$

Note that the elements of matrices $\mathbf{H}, \mathbf{G}, \mathbf{R}$ and $\mathbf{g}(\mathbf{x})$ depend only on geometrical data. Thus, they can all be computed once and stored.

III. THE PROPOSED LOCALLY ADAPTIVE-MULTIQUADRIC SHAPE

Regarding the studies in the search for the optimal choice of the shape parameter, many outstanding and well-known forms proposed in the past are listed in Table 1.

Table 1
Some Choices Proposed in Literature

Reference	Formulation of/for j^{th} -element
Kansa [11]	$\epsilon_j = \left[\epsilon_{\min}^2 \left(\frac{\epsilon_{\max}^2}{\epsilon_{\min}^2} \right)^{\frac{j-1}{N-1}} \right]^{\frac{1}{2}}$, with $j=1, 2, \dots, N$
Kansa and Carlson [12]	$\epsilon_j = \epsilon_{\min} + \left(\frac{\epsilon_{\max} - \epsilon_{\min}}{N-1} \right) j$, with $j=0, 1, 2, \dots, N-1$
Sarra [13]	$\epsilon_j = \epsilon_{\min} + (\epsilon_{\max} - \epsilon_{\min}) \times \text{rand}(1, N)$
Sarra and Sturgill [14]	$\epsilon_j = \frac{\mu}{h_n} [\epsilon_{\min} + (\epsilon_{\max} - \epsilon_{\min}) \times \text{rand}(1, N)]$

Here, the command 'rand' is the MATLAB function that returns uniformly distributed pseudo-random numbers on the unit interval. It was proven in Sarra and Sturgill [14] that the variable shape outperformed the fixed value of parameter

especially when the scheme includes the information about the minimum distance of a centre to its nearest neighbour, h_n , with also a user input value μ .

In this work, we propose a new form of variable shape parameter where both linear and exponential manners are taken into consideration, expressed as in Equations (28)-(30).

$$\varepsilon_j = (1-\zeta) \cdot \varepsilon_{\text{exp}} + \zeta \cdot \varepsilon_{\text{lin}} \quad (28)$$

where;

$$\varepsilon_{\text{exp}} = \left[\varepsilon_{\text{min}}^2 \left(\frac{\varepsilon_{\text{max}}^2}{\varepsilon_{\text{min}}^2} \right)^{\zeta} \right]^{\frac{1}{2}} \quad (29)$$

$$\varepsilon_{\text{lin}} = \left[\varepsilon_{\text{min}} + (\varepsilon_{\text{max}} - \varepsilon_{\text{min}}) \zeta \right] \quad (30)$$

and ζ is set to correspond to the local *Peclet* number defined as follows;

$$\zeta = \frac{Pe_{ij}}{\text{Max}_{i \neq j} |Pe_{ij}|} \quad (31)$$

And the dimensionless number called the Péclet number (Pe), which is the ratio of the contributions to mass transport by convection to those by diffusion is expressed as;

$$Pe = \frac{c_k |\mathbf{u}|}{D \nabla c_k} = \frac{LU}{D} \quad (32)$$

where L is a characteristic length scale and taken as the distance between the centre node i and the pointing node j . U is the local velocity magnitude, and D is a characteristic diffusion coefficient, i.e. ω_x and ω_y in Equation (3) and $j=1,2,\dots,N$. The automatically self-adjusted parameter ζ is introduced and act as a weight function leading ε_j to equal to the exponential manner when $j = 1$. This weight then sets ε_j to become its linear mode when $j = N$. This proposed variable shape is referred to as ‘**Var**’ throughout the work.

IV. NUMERICAL EXPERIMENT AND GENERAL DISCUSSION

In this section, we applied the method explained above to the steady state of the problem, the time-dependence term in Equation (3) is omitted. The domain is a unit square $(x, y) \in \Omega = [0,1] \times [0,1]$ and $V_x = 3-x, V_y = 4-y$ with constants $\omega_x = \omega_y = \omega$ and $\beta = 1$ and the source term are omitted. All four sides of the domain are set with the same boundary condition as $(0, y) = u(1, y) = u(x, 0) = u(x, 1) = 0$, leading to the exact solution as the following form, Gu and Liu [15];

$$u_{\text{exact}} = \sin(x) \left(1 - e^{-\frac{2(1-x)}{\omega}} \right) y^2 \left(1 - e^{-\frac{3(1-y)}{\omega}} \right) \quad (33)$$

For error analysis, the two error indicators, over the domain, are adopted in this work and are given by;

$$\text{Relative Error} = \left| \frac{u_i^{\text{exact}} - u_i^{\text{num}}}{u_i^{\text{exact}}} \right| \quad (34)$$

$$\text{Root Mean Square (RMS) error} = \sqrt{\frac{\sum_{i=1}^N (u_i^{\text{exact}} - u_i^{\text{num}})^2}{N}} \quad (35)$$

Table 2 and Table 3 show the RMS produced by using optimal ε for each value of ω at different node densities, 100 and 441 respectively. Moreover, in both tables, we show the influence of the wideness of the interval or the distance between the maximum and minimum of ε . The results from all the cases carried out here interestingly reveal that the optimal shape parameter is within the interval $\varepsilon \in (1.4, 1.7)$. To emphasise the effectiveness of the proposed formula, not being influenced by the range ε , we expanded the range from $(\varepsilon_{\text{min}}, \varepsilon_{\text{max}}) = (1, 10)$ to $(0.1, 20)$ and from $(0.1, 20)$ to $(0.01, 40)$. It is interestingly found that the optimal values still occur at nearly the same area of the value curve. All numerical solutions also behave in the same tendency when the value of ω gets smaller where the RMS is found to increase slightly. The relative error norm, Equation (34) is depicted in Figure 1 and clearly shows the optimal values of ε for both numbers of nodes involved.

Table 2
Numerical Solution Computed with 100 nodes (N+L), at Two Intervals of ε_{min} and ε_{max} , and at Different Values of ω .

ω	$(\varepsilon_{\text{min}}, \varepsilon_{\text{max}}) = (1, 10)$	
	Optimal Value	RMS
50	1.43E+00	3.01E-09
10	1.51E+00	6.59E-09
5	1.50E+00	6.25E-08
1	1.52E+00	2.03E-08
0.5	1.64E+00	2.56E-08
ω	$(\varepsilon_{\text{min}}, \varepsilon_{\text{max}}) = (0.1, 20)$	
	Optimal Value	RMS
50	1.50E+00	4.41E-09
10	1.54E+00	7.25E-09
5	1.39E+00	4.78E-08
1	1.45E+00	3.02E-08
0.5	1.55E+00	4.23E-07
ω	$(\varepsilon_{\text{min}}, \varepsilon_{\text{max}}) = (0.01, 40)$	
	Optimal Value	RMS
50	1.55E+00	5.21E-09
10	1.64E+00	5.20E-09
5	1.59E+00	4.12E-08
1	1.55E+00	4.42E-08
0.5	1.65E+00	6.02E-07

Table 3
Numerical Solution Computed with 441 nodes (N+L), at Two Intervals of \mathcal{E}_{\min} and \mathcal{E}_{\max} , and at Different Values of ω .

ω	$(\mathcal{E}_{\min}, \mathcal{E}_{\max}) = (1, 10)$	
	Optimal Value	RMS
50	1.47E+00	5.01E-09
10	1.45E+00	6.05E-09
5	1.56E+00	5.32E-09
1	1.51E+00	2.02E-08
0.5	1.62E+00	5.02E-08
ω	$(\mathcal{E}_{\min}, \mathcal{E}_{\max}) = (0.1, 20)$	
	Optimal Value	RMS
50	1.54E+00	3.01E-09
10	1.46E+00	5.88E-09
5	1.39E+00	5.98E-09
1	1.52E+00	1.26E-08
0.5	1.70E+00	2.47E-08
ω	$(\mathcal{E}_{\min}, \mathcal{E}_{\max}) = (0.01, 40)$	
	Optimal Value	RMS
50	1.49E+00	5.23E-09
10	1.58E+00	6.55E-09
5	1.42E+00	5.02E-08
1	1.58E+00	8.22E-08
0.5	1.68E+00	3.23E-07

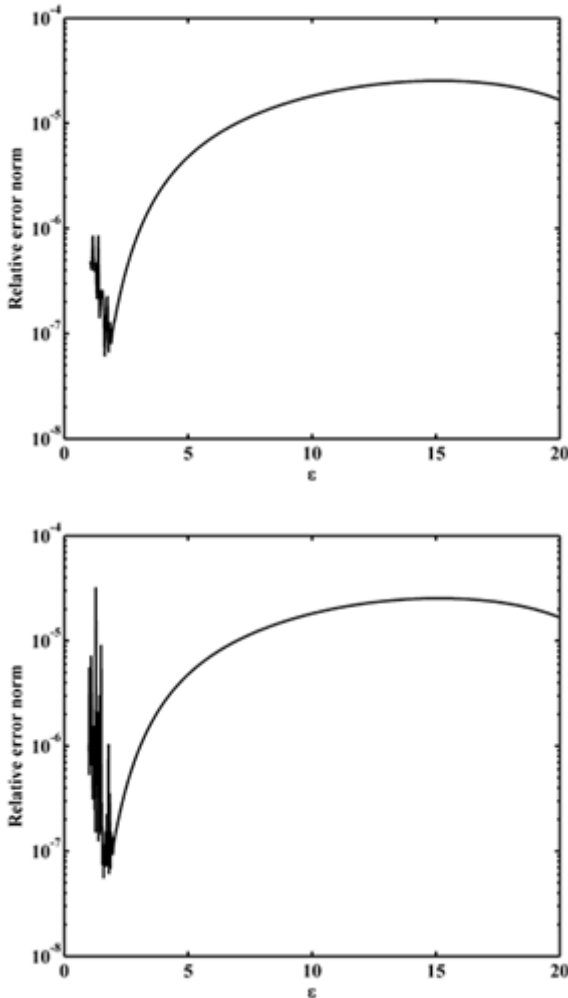


Figure 1: Relative error norm, Equation (34); above) computed with 100 nodes, and below) computed with 441 nodes (N+L) for $\omega = 0.1$.

In order to compare the results obtained in this study to one of the benchmarks in literature namely Gu and Liu [15], and also to some of our previous works, a new error indicator (Err), is adopted and defined as;

$$Err = \sqrt{\frac{\sum_{i=1}^N (u_i^{exact} - u_i^{num})^2}{\sum_{i=1}^N (u_i^{exact})^2}} \quad (36)$$

In one of our previous investigations, Chanthawara et al. [16], it was found that other kinds of radial basis functions rely on different values of optimal shape parameters. Here, we compare the error norm, Err , of the results obtained from this work to some other RBFs, with fixed \mathcal{E} . It is found that by using our proposed form of variable shape, Equation (28)-(30), satisfactory results can also be obtained. It is to be also mentioned that when the convection force becomes dominant, $\omega \leq 1$, the numerical method loses their effectiveness and this figure is known as normal, see Table 4.

Table 4
Comparison of Err at Different Levels of Convection Force, Computed at 400 Nodes (N+L)

ω	Gu and Liu ¹⁵	NAA* ($\mathcal{E} = 10$)	IMQ* ($\mathcal{E} = 0.01$)	Var (Opt. \mathcal{E})
100	0.245	0.435	0.990	0.448 ($\mathcal{E} = 1.48$)
10	0.255	0.371	0.912	0.901 ($\mathcal{E} = 1.56$)
1	0.346	0.589	3.849	1.525 ($\mathcal{E} = 1.59$)
0.1	1.276	38.307	15.417	8.769 ($\mathcal{E} = 1.61$)
0.01	15.832	1970.006	67.072	22.015 ($\mathcal{E} = 1.68$)

*Adopted from Chanthawara et al. [16]

Velocity solution profiles are plotted in Figure 2, and it can be seen that the solution obtained by using the locally-adaptive shape proposed in this work outperforms the one with fixed value.

V. CONCLUSION

In this work, we have studied the effectiveness of the fixed values of shape parameter contained in the Multiquadric type of RBFs, $\varphi(r, \mathcal{E}) = \sqrt{\mathcal{E}^2 + r^2}$, in conjunction with the method of DRBEM. The investigation began with applying DRBEM to one of the most complicated PDEs namely convection-diffusion type. We then proposed a new form of shape parameter that behaves locally-adaptive, i.e. it varies accordingly to the local change of the physics of the problem which, here, is the Peclet number (Pe). The proposed variable shape form also contains both linear and exponential aspects based on the distance between the centre node i and pointed node j in the RBF-collocation numerical method adopted. Some important conclusions can now be drawn from the investigation, and they are as follows:

- DRBEM has successfully been applied to convection-diffusion using multiquadric radial basis function at a wide range of convection force.
- It is found from all the results obtained in this work that the proposed shape parameter can outperform the fixed ones and certainly deserves further investigation.

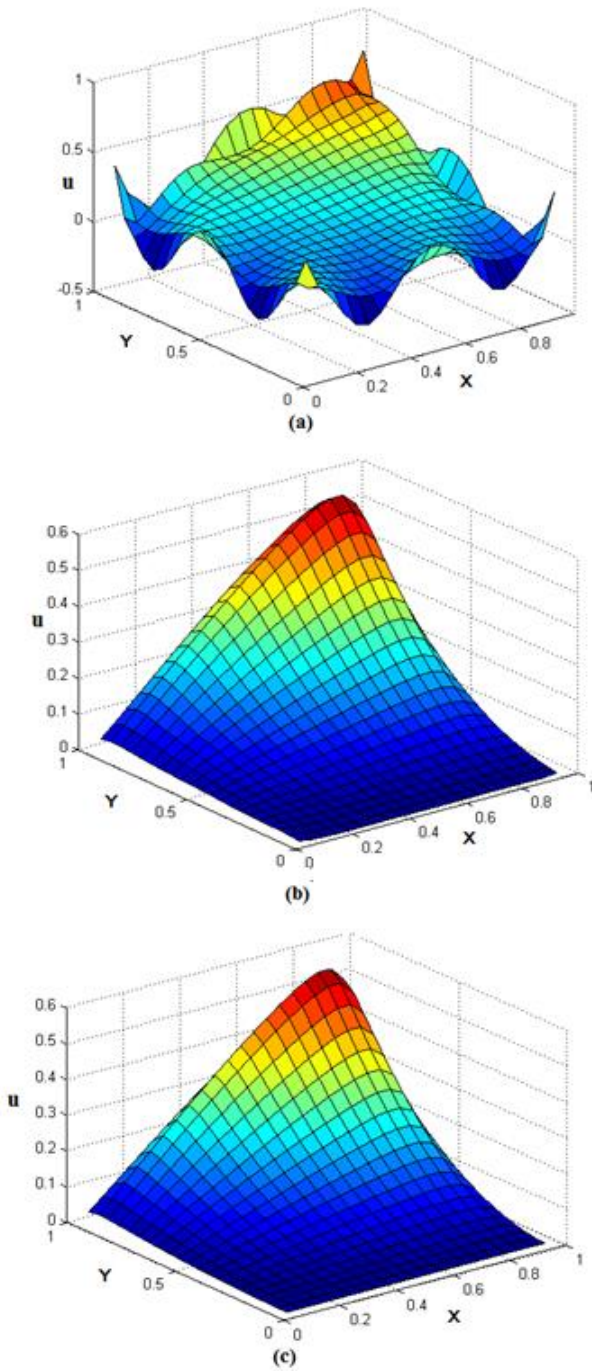


Figure 2: Numerical solution obtained from 21×21 nodes; (a) obtained with fixed shape $\varepsilon = 10$, (b) optimal shape found in this work, and (c) Exact solution, measured at $\omega = 0.1$

- When compared with other numerical works, the accuracy lies at an acceptable level but gets lower when the convection force is greater.

ACKNOWLEDGEMENTS

The corresponding author would like to express his sincere gratitude and appreciation to the Center of Excellence in Mathematics, Thailand for their financial support.

REFERENCES

- [1] C.A. Brebbia, R.L. Butterfield. Formal equivalence of direct and indirect boundary element methods. *Applied Mathematical Modelling*, 2(2)(1978) 132-134.
- [2] T.A. Foley, R.E. Carlson. The parameter R^2 in multiquadric interpolation. *Computers and Mathematics with Applications*, 21(9)(1991) 29-42.
- [3] R.L. Hardy. Multiquadric equations of topography and other irregular surfaces. *J. Geophys. Res.*, 76(8)(1971) 1905-1915.
- [4] C. Franke, R. Schaback. Convergence orders of meshless collocation methods using radial basis functions. *Adv Comput Math*, 93(1998) 73-82.
- [5] X. Zhang, K.Z. Song, M.W. Lu, X. Liu. Meshless methods based on collocation with radial basis functions. *Comput. Mech.*, 26(4)(2000) 333-343.
- [6] J.G. Wang, G.R. Liu. On the optimal shape parameters of radial basis functions used for 2-d meshless methods. *Meth. Appl. Mech.Eng.*, 191(23-24)(2002) 2611-2630.
- [7] C.K. Lee, X. Liu, S.C. Fan. Local multiquadric approximation for solving boundary value problems. *Comput. Mech.*, 30(5)(2003) 396-409.
- [8] K. Chanthawara, S. Kaennakham, W. Toutip. The dual reciprocity boundary element method(DRBEM) with multiquadric radial basis function for coupled burgers' equations'. *International Journal of Multiphysics*, 8(2)(2014) 123-143.
- [9] W. Toutip. *The Dual Reciprocity Boundary Element Method for linear and nonlinear problems*. PhD thesis, University of Hertfordshire, Hertfordshire, United Kingdom.
- [10] J. Duan, J. Nee. Limit Set of Trajectories of the Coupled Viscous Burgers Equations'. *Applied Mathematics Letters*, 11(1)(1998) 57-61.
- [11] E.J. Kansa. Multiquadrics{a scattered data approximation scheme with applications to computational fluid dynamics-I. *Comput. Math. Appl.*, 19(1990) 127-145.
- [12] E.J. Kansa, R.E. Carlson. Improved accuracy of multiquadric interpolation using variable shape parameters. *Comput. Math. Appl.*, 24(1992) 99-120.
- [13] S.A. Sarra. Adaptive radial basis function method for time dependent partial differential equations. *Appl. Num. Math.*, 54(2005) 79-94.
- [14] S.A. Sarra, D. Sturgill. A random variable shape parameter strategy for radial basis function approximation methods. *Engineering Analysis with Boundary Elements*, 33(11)(2009) 1239-1245.
- [15] Y.T. Gu, G.R. Liu. Meshless techniques for convection dominated problems. *Comput. Mech.*, 3(2)(2006) 171-182.
- [16] Chanthawara, K., Kaennakham, S. and Toutip, W., The Numerical Study and Comparison of Radial Basis Functions in Applications of the Dual Reciprocity Boundary Element Method to Convection-Diffusion Problems, *Progress in Applied Mathematics in Sciences and Engineering, AIP Conference Proceedings* 1705, 020029 (2016).